ISSN 1330-3651 (Print), ISSN 1848-6339 (Online)
Received: 23 April 2024; Accepted: 16 August 2025

https://doi.org/10.17559/TV-20240423001491
Original scientific paper

Corrosion Properties of Al_2O_3-TiO_2 Ceramic Coatings Deposited by Plasma Spraying on AZ91 Magnesium Alloy in Different Environment

Hüseyin ÖZKAVAK*, Recai Fatih TUNAY

Abstract: Magnesium and its alloys are used in many industrial fields and are the lightest material group among green materials, but it limits the usage area due to its low corrosion resistance. Surface coating methods are used to improve the corrosion properties. In this study, it was aimed to determine the corrosion behavior of AZ91 magnesium alloy in different corrosive environments (0.3 M H_2SO_4 and 3.5% NaCl). For this purpose, different ratios of Al_2O_3 and TiO_2 were coated on AZ91 Mg alloy using the Atmospheric Plasma Spray (APS) method. At the end of the study, the highest corrosion resistance was obtained in the 100% Al_2O_3 coated samples, and the corrosion rate in the 3.5% NaCl corrosive environment was higher than that of the 0.3 M H_2SO_4.

Keywords: APS; ceramic coating; corrosion; different corrosive enviroment; Mg alloy

1 INTRODUCTION

Magnesium alloys have started to take place as the lightest material group among green metallic materials in the 21st century. Magnesium alloys are used in the automobile and aerospace industries due to their low density and high specific strength and hardness, excellent castability, good electromagnetic shielding performances [1-3]. Although it has such superior properties, it has limited its use in many areas due to its low corrosion resistance [4, 5]. Alloying and surface coating methods are used to increase the corrosion resistance of magnesium alloys. Magnesium can be alloyed using some elements such as manganese, zinc, zirconium, and aluminum [4].

It is an effective method used to increase the corrosion resistance of magnesium and its alloys with the surface coating process, as well as to improve the surface hardness and wear resistance. Thermal spray processes such as Atmospheric Plasma Spray (APS), HVOF, and wire arc are used on light metal alloys to create such coatings [6]. In addition to metals and hard metals, ceramic materials are the most important material group in the preparation of thermal spray coating solutions [7]. APS is one of the most common methods used in the preparation of ceramic coatings due to its high melting temperatures [7]. TiO_2, Al_2O_3, and ZrO_2 ceramic coatings using the APS method find widespread use due to their excellent corrosion resistance in the seawater environment. Al_2O_3 ceramic coatings are widely used in industrial applications due to their high hardness and electrical resistance, good chemical stability, strong compatibility and low production cost, good mechanical properties, wear resistance, and anti-corrosion properties. Al_2O_3 ceramic material has a brittle structure. In the case of adding TiO_2 to Al_2O_3, the hardness of the coating is reduced and the toughness is increased [8-10]. Titanium oxide is another ceramic material that is frequently used due to its multifunctional character [7]. The use of TiO_2 in different applications is closely related to the existence of different TiO_2 modifications and the formation of lower oxides.

In addition, TiO_2 reduces porosity by increasing the corrosion resistance, wear resistance, and modulus of elasticity [11]. TiO_2 is a material with a low melting point and when added to Al_2O_3, it improves the coating performance by reducing the melting point of Al_2O_3 grains [12]. Al_2O_3-TiO_2 coatings are important because they can preserve the beneficial properties of TiO_2 and Al_2O_3 [13]. The addition of TiO_2 to Al_2O_3 improves fracture toughness [14], corrosion and wear resistance [15,16] , photocatalytic [17] and dielectric [18] properties. Due to all these properties, the examination of Al_2O_3- TiO_2 coatings has been the subject of many studies. Harju et al., in their study, investigated the effect of surface properties, surface tension, and phase inhomogeneity of TiO_2, Al_2O_3 based coatings [19]. Toma et al. investigated the corrosion behavior of Al_2O_3-TiO_2 coatings at different ratios (Al_2O_3; Al_2O_3- %3 TiO_2 and Al_2O_3- %40 TiO_2). It was determined that the corrosion resistance increased with the addition of TiO_2 [7]. In another study, it was determined that the melting of powders in Al_2O_3-TiO_2 coated samples is not solely dependent on the TiO_2 ratio, but also on the production of the powder [20]. In their study, Wang and Shaw stated that the fused and crushed raw material powder composed of separately fused Al_2O_3 and TiO_2 particles had better thermal conductivity than the agglomerated Al_2O_3 + TiO_2 powder [21]. Poor thermal conductivity led to an increase in the porosity of the coating. In this study, similar situations occurred, and as the TiO_2 ratio increased, the corrosion resistance decreased. Suopys et al., have studied coating Al_2O_3 on P265GH steel. In this work thermal and chemical resistance of coated steel were investigated by coating Al_2O_3-13%TiO_2. The coating process prevented the degradation of the substrate. It was determined that the uncoated steel material was heavily oxidized after 5 heat treatment cycles. After 20 thermal cycles, the thermal and chemical resistance of the Al_2O_3-coated samples increased [8]. Michalak et al. investigated the effect of TiO_2 on the tribological properties of samples coated with 3%, 13%, and 40% TiO_2. In the study, it was determined that the phases belonging to pure Al_2O_3 (α-Al_2O_3; γ-Al_2O_3) decreased and the TiO_2 phases (rutile-TiO_2, Al_2TiO_5) increased with the increase in TiO_2. In addition, the best tribological performance was obtained in samples coated with 13% TiO_2, in which a decrease in hardness occurred with an increase in TiO_2 [20]. Bahramian et al. determined in their study that the corrosion resistance of Al alloy increased by adding nanoparticle TiO_2 to the coating in the coating process using DC power [16].

When the literature is examined, it has been determined that there are not many studies on the corrosion properties of TiO_2-added coatings in different environments. In this study, besides 3%, 13%, 40% TiO_2 coatings, the corrosion behavior of the samples coated with Al_2O_3 and TiO_2 was determined in the environment of 3.5% NaCl and 0.3 M H_2SO_4. The results obtained from the study will guide the determination of coating parameters suitable for the usage area of Mg alloys, which are widely used.

2 MATERIALS AND METHODS

2.1 Materials and Coating Process

In the study, AZ91 alloy from VIG Metal Company in Turkey with the dimensions of 15 × 15 × 5 mm was used as the substrate. The chemical composition of the substrate is provided in Tab. 1. Al_2O_3 with a melting temperature of 2070 °C and TiO_2 powder material with a melting temperature of 1830 °C were used as coating materials. Al_2O_3 and TiO_2 powder materials of 40-80 µm size were mixed by ball milling method. One of the most important factors affecting the coating quality is the surface preparation of the substrate. For this reason, surface preparation processes were applied to AZ91 substrates. For this purpose, it is aimed to increase the adhesion resistance during coating by applying surface sandblasting and then ultrasonic cleaning to the samples. Then, Ni-Cr primer material was applied to the substrates in order to increase the coating bonding ability.

Sulzer Metco 9MB plasma spray system was used to prepare the coating. The coating of the samples and the images of the coated samples are provided in Fig. 1. The plasma spraying process parameters used in the study are the optimum parameters and are given in Tab. 2.

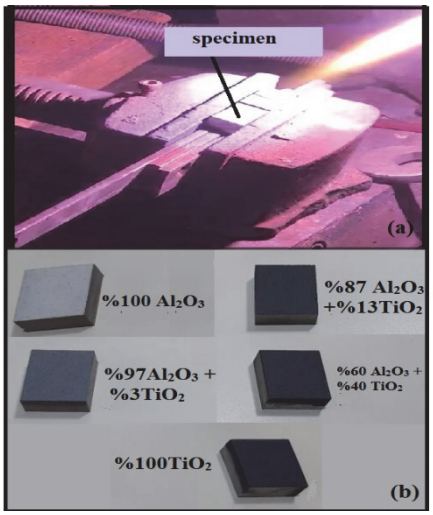

Figure 1 (a) Coating of the samples and (b) The images of the coated samples

Table 1 The chemical composition of the substrate (AZ91 Magnesium Alloy)

Alloying element	Al	Zn	Mn	Fe	Si	Cu	Mg
%	8.8	0.61	0.18	0.02	0.02	0.005	Balance

Table 2 Plasma spraying process parameters

Coating rates	Spraying distance / cm	Voltage / V	Current / A	Ar flow (SCFH)	H_2 flow (SCFH)	Powder feed rate / lb/h
TiO_2/Al_2O_3	9	69	580	83-90	125-135	3.78
3% TiO_2	8	60-62	570	86-92	130-137	3.5
13% TiO_2	7	58-60	550	86-90	120	4
40% TiO_2	6	55-58	530	83-90	125-135	3

2.2 Microstructural Investigations

X-ray diffraction (XRD) studies were performed using a Cu-α radiation source on the Bruker D8 Advance Twin-Twin device at room temperature. Data were collected at 2θ = 20-100°, 0.02° steps, and 0.3 s step time. Fei Quanto Feg 250 device was used for SEM and EDS analyses to determine the microstructure and phase composition of the coated samples before and after the corrosion tests.

2.3 Electrochemical Measurements

In the study, Gamry Reference 600 potentiostat/galvanostat device was used to determine the corrosion behavior of the coated samples and was characterized by Echem Analyst Soft software. In the study, corrosion tests were carried out in 3.5% NaCl and 0.3 M H_2SO_4 solutions at room temperature. The beakers were sealed to prevent the evaporation of the solutions. Corrosion tests were carried out in a 3-electrode system using Ag/AgCl reference electrode, 1 cm^2 Pt plate counter electrode, and sample as the working electrode. Scanning rate of 1 mV/s, polarization range of –0.25 V ± 0.25 V, and frequency of 20 Hz was chosen for the experiment. Before the corrosion tests, the coated samples were ultrasonically cleaned with acetone for 15 minutes, ethanol for 15 minutes and double-distilled water for 15 minutes at 35 °C, and then dried by keeping them in an oven at 50 °C for 1 hour. For potential measurements, each sample was kept in a solution of 3.5% NaCl and 0.3 M H_2SO_4 for 1 hour, allowing the system to reach equilibrium. Tafel plots were measured to determine the corrosion potential (Ecorr) and corrosion current density (Icorr). All electrochemical experiments were repeated 3 times.

3 RESULT AND DISCUSSION

3.1 Microstructural Analysis

SEM images of samples coated with varying ratios of Al_2O_3-TiO_2 on AZ91 substrate are shown in Fig. 2. It was observed that there are no defects between the substrate material and the coating material in the applied coatings, and that no defects were observed during the substrate coating process. The coating was applied in accordance with the general structure of ceramic cladding, indicating a uniform adhesion bond between the substrate material and the coating. Low porosity occurred in Al_2O_3-coated samples, whearas higher porosity was found in the TiO_2-

added coatings compared to the Al_2O_3 coatings. Previous studies have indicated that the TiO_2 ratio alone does not significantly influence the coating quality [20,21]. Furthermore, the nucleation of TiO_2 and the method of powder production also play a crucial role. In this study, a reduction in corrosion resistance was observed as the TiO_2 content increased. This decline is believed to be attributed to the increased porosity resulting from TiO_2 nucleation.

The coating thicknesses of the coated samples were measured and it was determined that the thickness values were obtained between 205 µm and 250 µm. In Fig. 3, XRD analyses of 100% Al_2O_3 and 100% TiO_2-coated samples are given. The phase structure of 100% Al_2O_3 coated samples was generally determined as α-Al_2O_3 phase. In addition, the presence of γ-alumina peaks draws attention. The reason for the formation of γ-Al_2O_3 peaks is the rapid solidification in the plasma spray method. It causes the formation of a reference nucleation phase with a low critical nucleation-free energy. Since γ-alumina has a low critical nucleation energy, it easily forms nucleation [22]. In addition, the formation of the metastable γ-Al_2O_3 phase, the melting rate of the ceramic particles, the sputtering rate, the particle distribution, and the heating of the substrate also caused the formation of the γ-Al_2O_3 phase. When the 100% TiO_2-coated samples were examined, anatase and rutile phases occurred in the structure. It has been determined that the dominant phase in the structure is the Rutile (210).

In Fig. 4, XRD analyses of 3%, 13%, and 40% TiO_2-coated samples are given. In samples coated with 3% TiO_2, the interphase is γ-Al_2O_3 and there are small amounts of α-Al_2O_3 and rutile-TiO_2 phases in this phase. The α-Al_2O_3 phase was formed as a result of rapid cooling and is consistent with the literature [10, 23, 24]. During the plasma coating process, the reaction between Al_2O_3 and TiO_2 resulted in the formation of the Al_2TiO_5 phase, which was also observed in the structure [7]. In samples coated with 13% TiO_2, α-Al_2O_3, γ-Al_2O_3, Al_2TiO_5, and rutile-TiO_2 phases were formed. It was determined that the addition of structural TiO_2 prevented the conversion from α-Al_2O_3 to γ-Al_2O_3. Additionally, the fact that the melting point of TiO_2 (1854 °C) is lower than that of α-Al_2O_3 (2010 °C) can be expressed as a reason for the presence of a small amount of untransformed α-Al_2O_3 still remaining in the structure [25]. This is in agreement with the literature [26-29].

Tucker et al. reported porosity values ranging from 5% to 15% in thermal spray coatings, while Fervel et al. observed values between 6% and 9%, and Michalak et al. found the range to be between 9% and 14% [30,31]. In the present study the porosity values were 8.98% for the %97 Al_2O_3 + 3% TiO_2 coated samples, 12.05% for the %87 Al_2O_3 + 13% TiO_2 coated samples, 13.01% for the %60 Al_2O_3 + 40% TiO_2 coated samples, 13.81% for the 100% TiO_2 coated samples, and 7.89% for the 100% Al_2O_3 coated samples. Furthermore, the presence of residual α-Al_2O_3 in the structure suggests the existence of unmelted or semi-melted particles within the coating [26-29]. This observation indicates that the unmelted or semi-melted particles contribute to the porosity in the coating structure.

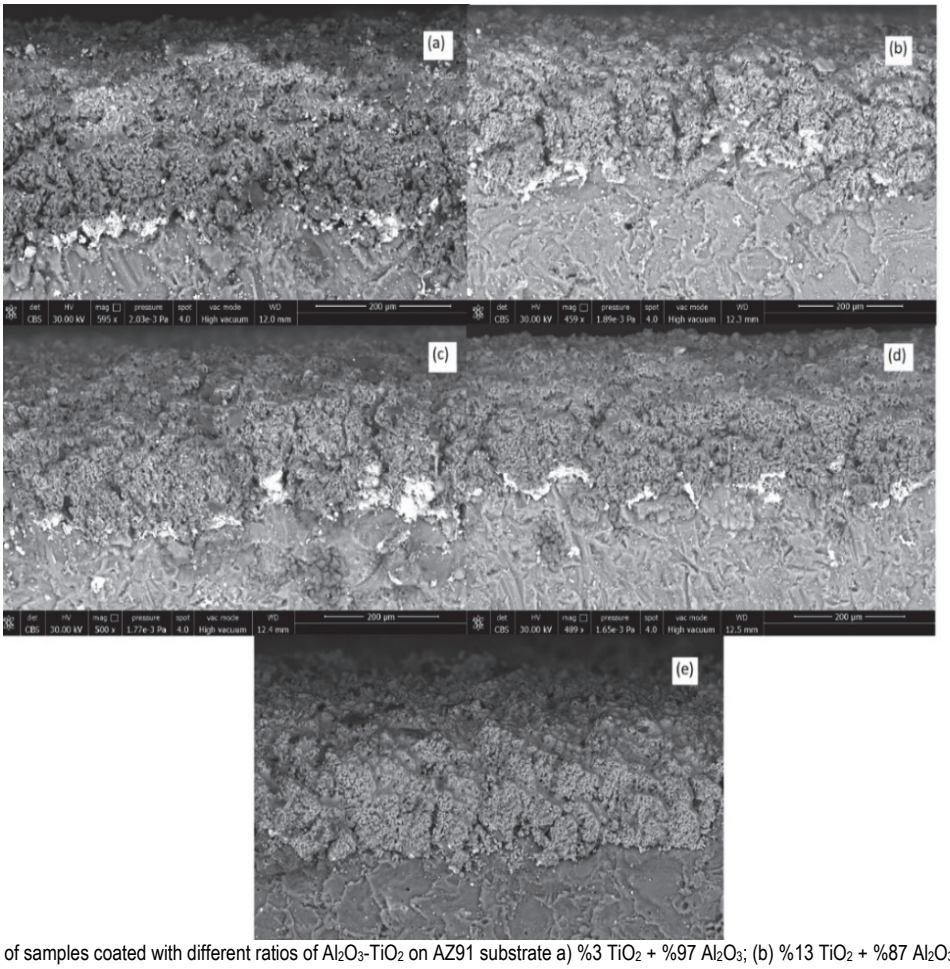

Figure 2 SEM images of samples coated with different ratios of Al_2O_3-TiO_2 on AZ91 substrate a) %3 TiO_2 + %97 Al_2O_3; (b) %13 TiO_2 + %87 Al_2O_3; (c) %40 TiO_2 + %60 Al_2O_3; (d) %100 TiO_2 (e) %100 Al_2O_3

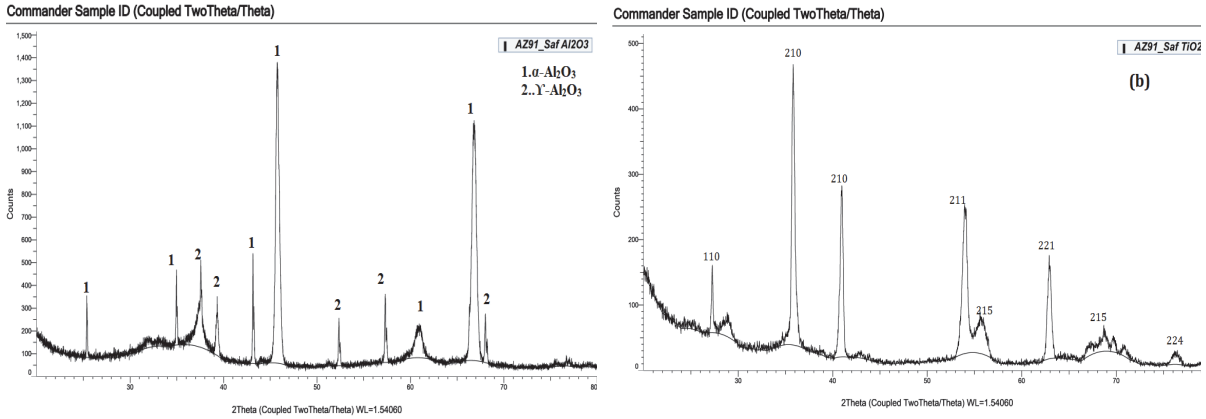

Figure 3 XRD analyses of (a)100% Al_2O_3 and (b)100% TiO2-coated samples

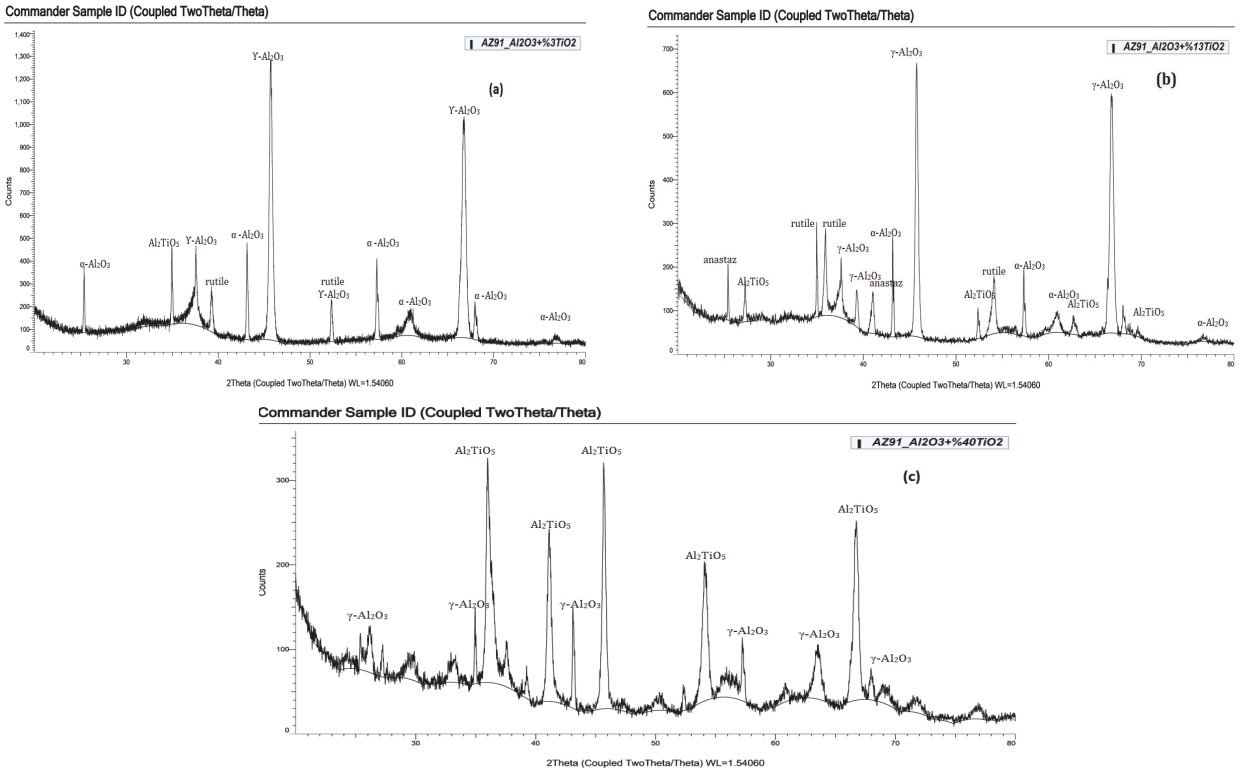

Figure 4 XRD analyses of (a) 3%; (b) 13%, and (c) 40% TiO_2-coated samples

3.2 Electrochemical Corrosion Results

In the study, corrosion tests were applied to samples coated with different ratios of Al_2O_3 - TiO_2 in different environments. The results of the applied potentiodynamic polarization tests are presented in Tab. 3. When the Ecorr values of the samples, which were subjected to corrosion tests in a 3.5% NaCl environment, were examined, the highest value was obtained in the 100% Al_2O_3 coated sample. This is due to the lower porosity of Al_2O_3 coatings. The presence of pores in the coating structure causes the substrate to be exposed to a corrosive environment. α-Al_2O_3 is a more stable phase and more resistant to corrosive environments. In 100% Al_2O_3 coated samples, the highest Ecorr value was obtained because the dominant phase was α-Al_2O_3. In the samples coated with 3%, 13%, and 40% TiO_2, the γ-Al_2O_3 phase was dominant and the α-Al_2O_3 phase was in small amounts, resulting in lower Ecorr values. When previous studies were examined, it was determined that γ-Al_2O_3 behaved less stable in corrosive environments than α-Al_2O_3 [19,22]. For this reason, it was determined that the samples coated with 3%, 13% and 40% TiO_2 show stability in corrosive environments.

The corrosion rates of the coatings in a 3.5% NaCl environment are presented in Tab. 3. Upon examining Tab. 3, it is observed that the lowest corrosion rate is 59.5 mpy for the 100% Al_2O_3 coated sample. This value increases to 75.77 mpy for the 3% Al_2O_3-TiO_2 coated samples, 90.28 mpy for the 13% Al_2O_3-TiO_2 coated samples, 183.77 mpy for the 40% Al_2O_3-TiO_2 coated samples, and 817.6 mpy for the 100% TiO_2 coated samples. The corrosion rate of the uncoated samples is 834.4 mpy. When compared with the uncoated samples, it is evident that the corrosion rates of the coated samples are significantly lower, indicating improved corrosion resistance. When the corrosion rates of the coatings in a 0.3 M H_2SO_4 environment were analyzed (Tab. 3), it was found that the lowest corrosion rate, 1.044 mpy, was observed in the 100% Al_2O_3 coated sample. This value increased to 32.36 mpy for the 3% Al_2O_3-TiO_2 coated samples, 91.69 mpy for the 13% Al_2O_3-TiO_2 coated

samples, 97.68 mpy for the 40% Al_2O_3-TiO_2 coated samples, and 219.2 mpy for the 100% TiO_2 coated samples. The corrosion rate of the uncoated samples was 934.4 mpy. The corrosion resistance of Al_2O_3 coated samples has shown better performance in both corrosive environments (3.5% NaCl and 0.3 M H_2SO_4). However, the addition of TiO2 resulted in an increase in porosity, which led to a rise in the corrosion rate.

Table 3 Corrosion data obtained by Tafel curves of TiO_2- Al_2O_3 coated with different rates in 3.5% NaCl and 0.3 M H_2SO_4 environment

Solution	Coating rates	Ecorr / mV	Icorr / µA	β_C	β_A	Corrosion Rate / mpy
3.5% NaCl	3% TiO_2	–1.4	91.4	509.7	15.9	75.77
0.3 M H_2SO_4		161	36.9	344.1	119.2	32.36
3.5% NaCl	13% TiO_2	–1.46	15.1	79.9	57.8	90.28
0.3 M H_2SO_4		–1.18	61.4	141.1	170.4	91.69
3.5% NaCl	40% TiO_2	–1.43	175	469.1	100.6	183.7
0.3 M H_2SO_4		–914	48	1	325	97.68
3.5% NaCl	100% TiO_2	–1.37	559	98.9	108.4	817.6
0.3 M H_2SO_4		–1.12	265	598.3	6.299	219.2
3.5% NaCl	100% Al_2O_3	–1.38	37	238.4	293.1	59.5
0.3 M H_2SO_4		–340	1.14	394.	286.8	1.044
3.5% NaCl	Non coated	–1.51	190	1	30.8	834.4
0.3 M H_2SO_4		–1.57	990	384	171.2	934.4

In Fig. 5, the potentiodynamic curves of the coatings made in a 3.5% NaCl environment are given. The passivation zone is clearly visible in the potentiodynamic curves of the substrate and 100% TiO_2-coated samples. It has been reported in the literature that the accumulation of cracks, which occurs at high apertures during the nucleation of the TiO_2 film, was reduced [32]. Consequently, as the TiO_2 content in the structure increased, a decrease in the fracture resistance of the coated samples in corrosive environments was observed.

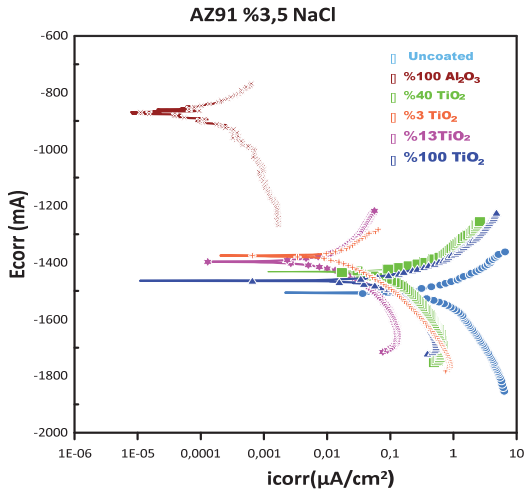

Figure 5 Potentiodynamics polarization curves for coatings in 3.5% NaCl environment

Mg and its alloys are chemically active and highly susceptible to corrosion in acid, neutral, or weak alkaline solutions [33]. Tafel polarization curves drawn after corrosion tests in a 0.3 M H_2SO_4 environment are given in Fig. 6. The plotted curves are in accordance with Tab. 3. It was observed that the corrosion potential shifted towards the positive value after the coating process. In addition, it was determined that the anodic current density values of the coated samples decreased somewhat compared to the uncoated samples.

When the Icorr values of the samples, which were subjected to corrosion tests in 0.3 M H_2SO_4 solution, were examined, the highest value was obtained in the uncoated samples. There was a decrease in Icorr values after coating. The lowest value was obtained in 100% Al_2O_3-coated samples. Similarly, when the corrosion rates in 0.3 M H_2SO_4 environment were examined, the highest value was obtained in the uncoated sample, while the lowest value was obtained in the 100% Al_2O_3 coated sample. Although the addition of TiO_2 to the coating material reduces the corrosion rate, it has been determined that a significant increase in corrosion resistance occurs compared to the uncoated samples. The addition of TiO_2 increased the porosity of the coating structure. This resulted in a decrease in the corrosion resistance.

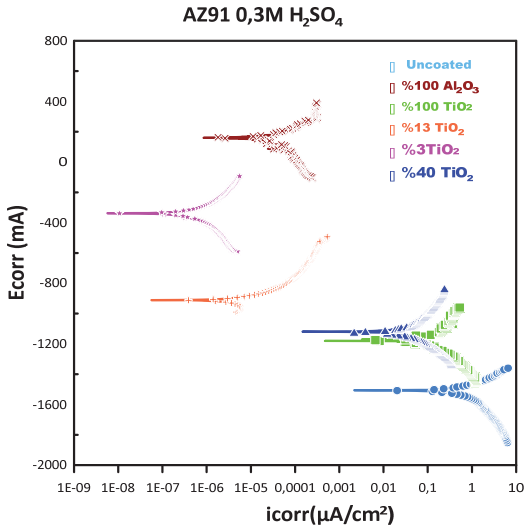

Figure 6 Potentiodynamics polarization curves for coatings in 0.3 M H_2SO_4 environment

The corrosion potantials of samples exposed to corrosion in a 0.3 M H_2SO_4 enviroment and the corrosion potantials in a 3.5% NaCl enviroment are given in Fig. 7. When the figure is examined, the corrosion potentials (Ecorr) of the samples in the 0.3 M H_2SO_4 environment were higher than in the 3.5% NaCl environment. It is due to the accelerated degradation of the coating film by Cl^- [34]. Furthermore, it is believed that solutions containing SO_4 have less impact on the AZ91 substrate material compared to solutions containing Cl-.

In the 3.5% NaCl environment of 100% Al_2O_3 coated samples, a low rate of dissolution occurs without forming a passive film on the surface (Fig. 5). A similar situation was obtained in samples coated with 100% TiO_2. It was determined that the corrosion rates of the samples coated

with 3% TiO_2 in a 3.5% NaCl medium were 2.4 times higher than the corrosion rates in 0.3 M H_2SO_4 medium. This value was determined as 1.7 times in 40% TiO_2-coated samples. Mg, a passive metal, is more prone to pitting corrosion in the presence of Cl^- ions in the absence of oxidizers [35]. The oxide film formed on the surface of Mg alloys is discontinuous and provides the formation of adsorption sites for anions such as Cl^-. Adsorption of Cl^- ions occurs in the α phase adjacent to the AlMn particles. At the self-occurring corrosion potential (1.53 V/SCE), the passivation film breaks and the α phase begins to dissolve and initiates pitting corrosion. Here, the α-Mg phase acts as the anode, while the AlMn particles in the pit act as the cathode.

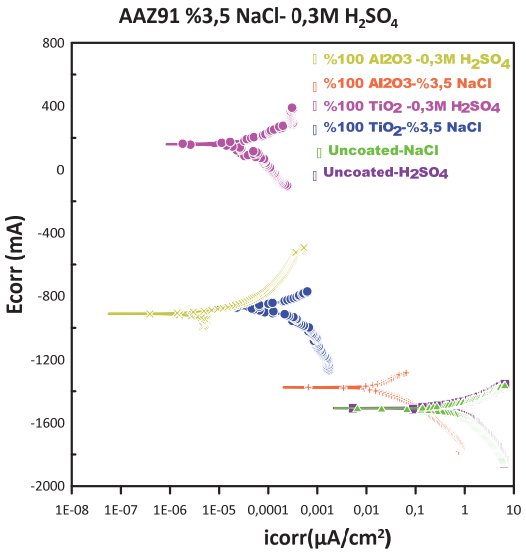

Figure 7 Potentiodynamics polarization curves for coatings in 3.5% NaCl and 0.3 M H_2SO_4 environments

Post-corrosion SEM examinations and EDS analyses of the samples in a 3.5% NaCl environment were performed and are given in Fig. 8. Upon reviewing studies on the effect of the Al content in Mg alloys on oxidation behavior, it has been determined that alloying Mg with Al leads to changes in both the oxide film on the surface and the microstructure, which reduces the disruptive effect of Cl- ions in aggressive environments. As a result, Al_2O_3, which is highly enriched in Al, provides a protective effect on the surface of the Mg alloy [36, 37]. A similar result was obtained in this study, where the 100% Al_2O_3 coated samples exhibited higher corrosion resistance. The addition of TiO_2 increased the porosity and accordingly the corrosion rate in 40% TiO_2-coated samples (Fig. 8c). In the EDS analysis of 40% TiO_2 coated samples, it was determined that there was an increase in the ratio of Ti and O in the structure. It has been determined that Ti and O form TiO and TiO_2 compounds in the structure, causing the structure to become heterogeneous and increase the corrosion rate. When the 100% TiO_2-coated samples were examined, it was clearly observed that the structure was highly porous (Fig. 8d).

SEM examinations after corrosion tests in 0.3 M H_2SO_4 solution are given in Fig. 9. When the figure was examined, it was determined that the coating significantly reduced the corrosion. In addition, it was determined that as the TiO_2 ratio in the structure increased, the cracks on the material surface due to corrosion increased. This is in agreement with the Tafel curves. The most important factor affecting the corrosion behavior of AZ91 Mg alloys, the β phase, which is the second phase and is present in the structure, is the morphology of this phase. As the Al ratio increases in the AZ91 alloy, the β-phase acts as a cathode according to the matrix structure and affects the corrosion. Increasing the β phase increases corrosion resistance by showing a barrier effect [38, 39].

The higher β phase formation in 100% Al_2O_3 coated samples resulted in an increase in corrosion resistance. In addition, Al_2O_3 is the most used ceramic to prevent corrosion due to its uniformity and good adhesion to the surface. Al_2O_3 nucleates well on metals and creates low porosity. By adding TiO_2 to the structure, it caused a decrease in corrosion resistance by creating porosity in the structure. For this reason, as the % TiO_2 ratio increased, the formation of cracks and pits in the structure increased. Furthermore, the literature indicates that in Al_2O_3-TiO_2 coated samples, the melting of the powders is not solely dependent on the Ti ratio but also on the powder production process, and that low thermal conductivity leads to an increase in coating porosity. This situation can be expressed as the reason for the decrease in corrosion resistance observed with the increase in TiO_2 ratio in this study [20, 21].

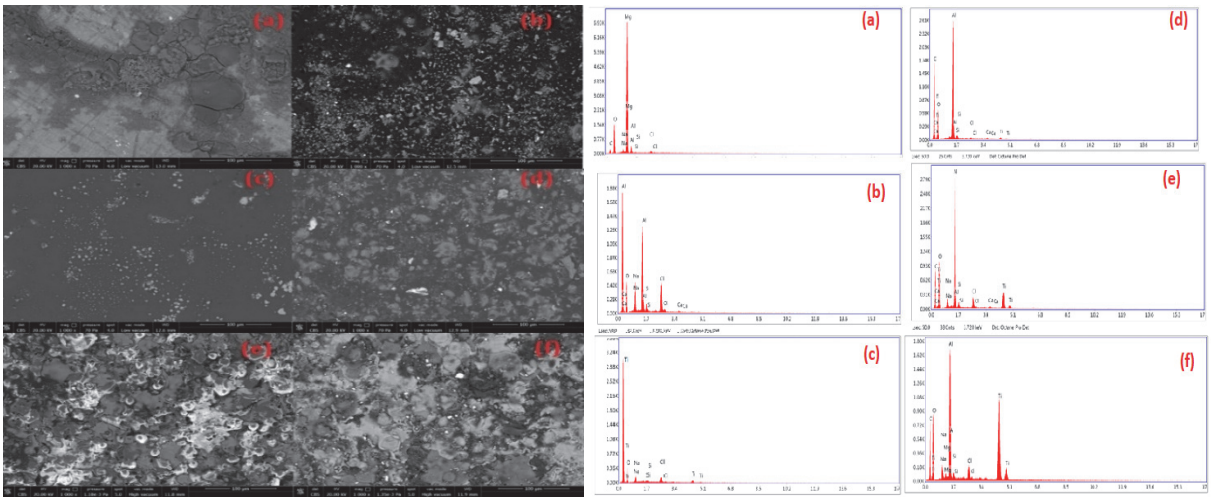

Figure 8 Post-corrosion SEM examinations and EDS analyses of the samples in a 3.5% NaCl environment (a) Uncoated; (b) %100 Al_2O_3; (c) %100 TiO_2; (d) %3 TiO_2; (e) %13 TiO_2; (f) %40 TiO_2

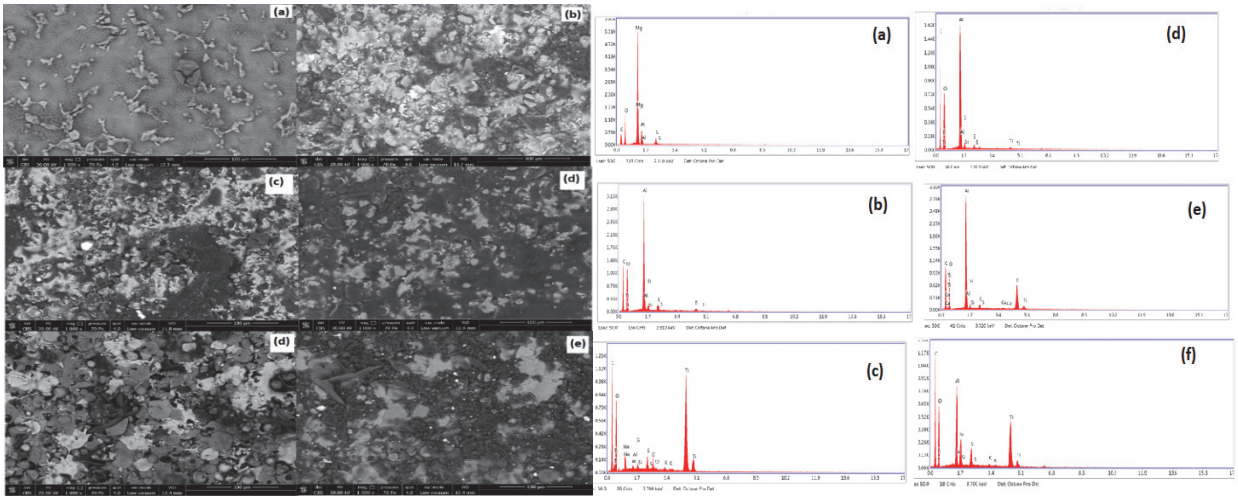

Figure 9 Post-corrosion SEM examinations and EDS analyses of the samples in a 0.3 M H_2SO_4 environment (a) Uncoated; (b) %100 Al_2O_3; (c) %100 TiO_2; (d) %3 TiO_2; (e) %13 TiO_2; (f) %40 TiO_2

4 CONCLUSIONS

In this study, the corrosion behavior of samples APS coated with different ratios of TiO_2 and Al_2O_3 on AZ91 alloy in different corrosive environments was investigated. The results obtained from the study can be summarized as follows:

- The uncoated samples exhibited the lowest corrosion resistance in both 3.5% NaCl and 0.3 M H_2SO_4 environments.
- It was observed that the corrosion resistance of the samples increased as a result of the coating process.
- The highest corrosion resistance was achieved with the 100% Al_2O_3-coated samples.
- An increase in the TiO_2 content in the coating structure led to a decrease in corrosion resistance, which can be attributed to the increased porosity within the structure.
- When comparing the 0.3 M H_2SO_4 and 3.5% NaCl environments, the samples exposed to the 3.5% NaCl environment exhibited higher corrosion rate than those exposed to the 0.3 M H_2SO_4 environment.

To check previous - Corrosion rates are lower in

Furthermore, to respond on the given suggestion - "In addition, TiO_2 reduces porosity by increasing the corrosion resistance, wear resistance, and modulus of elasticity [12]".; "Toma et al. investigated the corrosion behavior of Al_2O_3-TiO_2 coatings at different ratios (Al_2O_3; Al_2O_3-%3 TiO_2 and Al_2O_3-%40 TiO_2). It was determined that the corrosion resistance increased with the addition of TiO_2 [8]". - In the Conclusions section, the comparison to the cited researches should be made - in your investigation, the addition of TiO_2 increases the porosity and decreases the corrosion resistance and in the mentioned researches, the situation is just opposite - to explain why is that.

Acknowledgements

This work was supported by the Scientific Research Projects Coordination Unit of Süleyman Demirel University within the scope of project number FDK-2019-7386.

5 REFERENCES

[1] He, S. M., Zeng, X., Peng, L. M., Gao, X., Nie, J. F., & Ding, W. J. (2007). Microstructure and strengthening mechanism of high strength Mg-10Gd-2Y-0.5 Zr alloy. *Journal of Alloy Compounds*, *427*(1), 316-323. https://doi.org/10.1016/j.jallcom.2006.03.015

[2] Kojima, Y. (2001). Project of platform science and technology for advanced magnesium alloys. *Materials Transactions*, *42*, 1154-1159. https://doi.org/10.2320/matertrans.42.1154

[3] Mordike, B. L. & Ebert, T. (2001).Magnesium properties-application-potential. *Materials Science Engineering A*, *302*, 37-45. https://doi.org/10.1016/S0921-5093(00)01351-4

[4] Shi, Z., Song, G., & Atrens, A. (2005). Influence of the β phase on the corrosion performance of anodised coatings on magnesium-aluminium alloys. *Corrosion Science*, *47*, 2760-2777. https://doi.org/10.1016/j.corsci.2004.11.004

[5] Song, G. & St John, D. (2004). Corrosion behaviour of magnesium in ethylene glycol. *Corrosion Science*, *46*, 381-1399. https://doi.org/10.1016/j.corsci.2003.10.008

[6] Ernst, P. & Fletcher, K. (2011). SUMEBore - thermally sprayed protective coatings for cylinder liner surfaces, 1-12.

[7] Toma, F., Stahr, C. C., Berger, L. M., Saaro, S., Herrmann, M., Deska, D., & Micheal, G. (2009). Corrosion Resistance of APS and HVOF Sprayed Coatings in the Al_2O_3-TiO_2 System. *Journal of Thermal Spray Technology*, *19*, 137-147. https://doi.org/10.1007/s11666-009-9422-2

[8] Šuopys, A., Marcinauskas, L., Kėželis, R., Aikas, M., & Uscila, R. (2020). Thermal And Chemical Resistance ofPlasma Sprayed Al_2O_3, Al_2O_3-TiO_2 Coatings. *Research Square preprint.* https://doi.org/10.21203/rs.3.rs-18422/v2

[9] Basha Ga, M. T., Srikantha, A., & Venkateshwarlua, B. (2020). A Critical Review on Nano structured Coatings for Alumina-Titania (Al_2O_3-TiO_2) Deposited by Air Plasma Spraying Process (APS). *Materials Today: Proceedings*, *22*, 1554-1562. https://doi.org/10.1016/j.matpr.2020.02.117

[10] Dejang, N., Watcharapasorn, A., Wirojupatump, S., Niranatlumpong, P., & Jiansirisomboon, S. (2010). Fabrication and Properties of Plasma-Sprayed Al_2O_3/TiO_2 Composite Coatings: A Role of Nano-Sized TiO_2 Addition. *Surfaces and Coatings Techology*, *204*, 1651-1657. https://doi.org/10.1016/j.surfcoat.2009.10.052

[11] Klyatskina, E., Espinosa, L., Darut, G., Segovia-López, F., Salvador, M. D., Montavon, G., & Agorges, H. (2015). Sliding wear behavior of Al_2O_3-TiO_2 coatings fabricated by the suspension plasma spraying technique. *Tribology Letters*, *59*(8), 1-9. https://doi.org/10.1007/s11249-015-0530-5

[12] Buytoz, S., Ersöz, E., Islak, S., Orhan, N., Kurt, B., & Somunkıran, İ. (2012). Microstructural Characteristics of Al_2O_3-TiO_2 Composite Coatings Produced by the Plasma Spray Method. *International Iron and Steel Symposium*.

[13] Li, H., Song, R., & Ji, Z. (2013). Effects of nano-additive TiO_2 on performance of micro-arc oxidation coatings formed on 6063 aluminum alloy. *Transactions of Nonferrous Metals Society of China*, *23*, 406-411. https://doi.org/10.1016/S1003-6326(13)62477-2

[14] Ra,j V. & Mumjıtha, M. (2014). Comparative study of formation and corrosion performance of porous alumina and ceramic nanorods formed in different electrolytes by anodization. *Materials Science and Engineering B*, *179*, 25-35. https://doi.org/10.1016/j.mseb.2013.10.001

[15] Song, R. G., Wang, C., Jıang, Y., Li H., Lu G., & Wang, Z. X. (2012). Microstructure and properties of Al_2O_3/TiO_2 nanostructured ceramic composite coatings prepared by plasma spraying. *Journal of Alloys and Compounds*, *544*, 13-18. https://doi.org/10.1007/s11666-021-01170-6

[16] Bahramıan, A., Raeıssı, K., & Hakımızad, A. (2015) An investigation of the characteristics of Al_2O_3/TiO_2 PEO nanocomposite coating. *Applied Surface Science*, *351*, 13-26. https://doi.org/10.1016/j.apsusc.2015.05.107

[17] Ignjatovıć, S., Blawert, C., Serdechnova, M., Karpushenkov, S., Damjanovıć, M., Karlova, P., Wıeland, D. C. F., Starykevıch, M., Stojanovıć, S., Damjanovıć-Vasılıć, L. J., & Zheludkevıc, M . (2021). Formation of multi-functional TiO_2 surfaces on AA2024 alloy using plasma electrolytic oxidation. *Applied Surface Science*, *544*, 148875. https://doi.org/10.1016/j.apsusc.2020.148875

[18] Campos, R. V., Bezerra, C. L., Olıveıra, L. N. L., & Gouveıa, D. X. (2015). A study of the dielectric properties of Al_2O_3-TiO_2 composite in the microwave and RF regions. *Journal of Electronic Materials*, *44*, 4220-4226. https://doi.org/10.1007/s11664-015-3958-3

[19] Harju, M., Halme, J., Järn, M., Rosenholm, J. B., & Mäntylä, T. (2007). Influence of Aqueous Aging on Surface Properties of Plasma Sprayed Oxide Coatings. *Journal of Colloid and Interface Science*, *313*(1), 194-201. https://doi.org/10.1016/j.jcis.2007.04.044

[20] Mıchalak, M., Latka, L., Sokolowskı, P., Candıdato, R. T., & Ambrozıak, A. (2021). Effect of TiO_2 on the microstructure and phase composition of Al_2O_3 and Al_2O_3-TiO_2 APS sprayed coatings. *Bulletın of the Polısh Academy of Sciences Technical Sciences*, *69*(2), e136735. https://doi.org/10.24425/bpasts.2021.136735

[21] Wang, M. & Shaw, L. (2007).Effects of the powder manufacturing method on microstructure and wear performance of plasma sprayed alumina-titania coatings. *Surface and Coatings Technol*ogy, *202*(1), 34-44. https://doi.org/10.1016/j.surfcoat.2007.04.057

[22] Gao, Y., Jie, M., & Liu, Y. (2017).Mechanical Properties of Al_2O_3 Ceramic Coatings Prepared by Plasma Spraying on Magnesium Alloy. *Surface and Coatings Technology*, *315*, 214-219. https://doi.org/10.1016/j.surfcoat.2017.02.026

[23] Varol Özkavak, H. & Asıl Uğurlu, H. (2022). Coating TiO_2 Film Using the Spin Method of AISI 304 Stainless Steel and Investigation of the Structural Properties. *International Journal of Innovative Engineering Applications*, 6(1), 97-102. https://doi.org/10.46460/ijiea.1070575

[24] McPherson, R.(1973). Formation of Metastable Phases in Flame- and Plasma-Prepared Alumina. *Journal of Materials Science*, *8*, 851-858. https://doi.org/10.1007/bf00553735

[25] Shaw, L. L., Goberma, D., Ren, R., Gell, M., Jiang, S., & Wang, Y. (2000). The Dependency of Microstructure and Properties of Nanostructured Coatings on Plasma Spray Conditions. *Surface and Coating Technology*, *13*, 1-8. https://doi.org/10.1016/S0257-8972(00)00673-3

[26] Pantelis, D. I. & Psyllaki, P. (2000). Tribological Behavior of Plasma Sprayed Al_2O_3 Coatings Under Severe Wear Conditions. *Wear*, *237*(2), 197-204. https://doi.org/10.1016/S0043-1648(99)00324-5

[27] Normand, B., Fervel, V., Coddet, C., & Nikitine, V. (2000). Tribological properties of plasma sprayed alumina-titania coating: role and control of microstructure. *Surface and Coating Technology*, *123*, 278-287. https://doi.org/10.1016/S0257-8972(00)00702-7

[28] Luo, H., Goberman, D., Shaw, L., & Gell, M. (2003). Indentation fracture behaviour of plasma-sprayed nanostructured Al_2O_3-13 wt.%TiO_2 coatings. *Materials Science and Engineering A*, *346*, 237- 245. https://doi.org/10.1016/S0921-5093(02)00523-3

[29] Lin, X., Zeng, Y., Zhou, X., & Ding, C. (2003). Microstructure of alumina - 3 wt.% titania coatings by plasma spraying with nonostructured powders. *Material Science Engineering A*, *357*, 228-234. https://doi.org/0000-0002-8175-6744

[30] Tucker, R. C. & Price, M. O. (1988). The effect of angle of deposition on the properties of selected detonation gun coatings. *Proceedings of the International Symposium on Advanced Thermal Spraying Technology and Allied Coatings*, 61-71.

[31] Fervel, V., Normand, B., & Coddet, C. (1999). Tribological behaviour of plasma sprayed Al_2O_3-based cermet coating. *Wear*, *230*, 70-77. https://doi.org/10.1016/S0043-1648(99)00096-4

[32] Zhao, M. C., Liu, M., Song, G., & Atrens, A. (2008). Influence of the β-phase morphology on the corrosion of mg alloy AZ91. *Corrosion Science*, *50*, 939-1953.

[33] Bard, A. J. & Faulkner, L. R. (2000). *Electrochemical methods: fundamentals and applications*. John Wiley and Sons, New York.

[34] Song, G., Atrens, A., John , DSt., Wut, X., & Naırn, J. (1997). The anodic dissolution of magnesium in chloride and sulphate solutions. *Corrosion Science*, *39*(1), 1981-2004. https://doi.org/10.1016/S0010-938X(97)00090-5

[35] Song, G. & Atrens, A. (2003). Understanding magnesium corrosion - a framework for ımproved alloy performance. *Advanced Engineering Material*, *5*, 837-858. https://doi.org/10.1002/adem.200310405

[36] Song, G. & Atrens, A. (1999). Corrosion mechanisms of magnesium alloy. *Advanced Engineering Materials*, *1*(1),11-33.

[37] Esmaily, M., Blucher, D. B., Svensson, J. E., Halvarsson, M., & Johansson, L. G. (2012). New insights into the corrosion of magnesium alloys -the role of aluminum. *Scripta Materialia*, *115*, 91-95. https://doi.org/10.1016/j.scriptamat.2016.01.008

[38] Froes, F. H., Kim, Y. W., & Hehmann, F. (1987). Rapid solidification of Aluminium, Magnesium and Titanium. *Journal of Metals*, *39*(8), 14-21. https://doi.org/10.1007/BF03258603

[39] Lunder, O., Lein, J. E., Aune, T. K., & Nisancioglu, K. (1989). The role of magnesium aluminuim (Mg17Al12) phase in the corrosion of magnesium alloy AZ91. *Journal Corrosion*, *45*(9), 741-748. https://doi.org/10.5006/1.3585029

Contact information:

Hüseyin ÖZKAVAK
(Corresponding author)
Isparta University of Applied Sciences, Isparta OSB Vocational School,
Department of Mechanical and Metal Technology,
Isparta, 32092, Turkey
E-mail: huseyinozkavak@isparta.edu.tr

Recai Fatih TUNAY
Süleyman Demirel University,
Faculty of Engineering, Department of Mechanical Engineering,
Isparta, 32200, Turkey
E-mail: recaitunay@sdu.edu.tr